Monolithic integration of well-ordered nanoporous structures in the microfluidic channels for bioseparation

Chiung-Wen Kuo [a,b], Jau-Ye Shiu [a], Kung Hwa Wei [b], Peilin Chen [a,*]

[a] Research Center for Applied Sciences, Academia Sinica, 128, Section 2, Academia Road, Nankang, Taipei 115, Taiwan
[b] Department of Material Science and Engineering, National Chiao Tung University, Hsin Chu 300, Taiwan

Available online 27 June 2007

Abstract

Gel electrophoresis and capillary gel electrophoresis are widely used for the separation of biomolecules. With increasing demand in the miniaturized devices such as lab-on-a-chip, it is necessary to integrate such a separation component into a chip format. Here, we describe a simple approach to fabricate robust three-dimensional periodic porous nanostructures inside the microchannels for the separation of DNA molecules. In our approach, the colloidal crystals were first grown inside the microchannel using evaporation assisted self-assembly process. Then the void spaces among the colloidal crystals were filled with epoxy-based negative tone photoresist (SU-8). UV radiation was used to cure the photoresist at the desired area inside the microchannel. After subsequent development and nanoparticle removal, the well-ordered nanoporous structures inside the microchannel were obtained. Our results indicated that it was possible to construct periodic porous nanostructures inside the microchannels with cavity size around 300 nm and interconnecting pores around 30 nm. The mobility of large DNA molecules with different sizes was measured as a function of the applied electric field in the nanoporous materials. It was also demonstrated that 1 kilo-base pair (kbp) DNA ladders could be separated in such an integrated system within 10 min under moderate electric field.
© 2007 Published by Elsevier B.V.

Keywords: Colloidal crystal; DNA separation; Microchip; SU-8; Inverse opal; Self-assembly

1. Introduction

There have been increased demands in the development of miniaturized total chemical analysis system where chemical or biological samples can be manipulated, separated and analyzed in an integrated system. Such an integrated microdevice provides a very powerful platform for investigating chemical and biological reactions with many advantages including minimal sample size, fast reaction time, low cost, and portability [1–5]. One of the major applications for the integrated microsystem is the separation of biomolecules where limited amounts of samples are available and multiple sample processing steps are required [6]. However, most of the separation components for nucleic acids and proteins used in the microchips still relied on gel or polymer solutions, which suffered from several drawbacks including insufficient size control in the nanometer scale, less mechanical robustness and non-standard integration process [7–9]. With recent advances in nanotechnology, several

artificial sieving nanostructures with well-controlled topology have been demonstrated capable of separating biomolecules [10–15]. However, sophisticated tools are required to construct well-controlled nanostructures inside the microchips and the fabrication processes were often time-consuming. Therefore, an alternative approach is badly needed for the fabrication of size-controlled nanostructures inside the microfluidic system.

Recently, the colloidal particles have been utilized to construct three-dimensional periodic nanostructures by the self-assembly process [16]. These self-assembled opaline lattices of colloidal particles provided a simple but fast approach to produce size-controlled nanostructures over a large area. In order to integrate the colloidal crystals into the microfluidic system, Ozin and coworkers [17–19] have employed evaporation-induced self-assembly to grow colloidal crystals inside the microchannels, which allowed easy integration with other microfluidic components. In our group, we have developed an addressable microfluidic system to create colloidal crystals at any desired area inside one- or two-dimensional microfluidic system using electrocapillary effect [20,21]. It was also shown that the colloidal crystals formed by different sizes of nanoparticles could be integrated into a single microchannel. In addition to the unique

* Corresponding author. Tel.: +886 2 2789 8000; fax: +886 2 2782 6680.
  E-mail address: peilin@gate.sinica.edu.tw (P. Chen).

optical properties exhibited by the well-ordered nanoparticles, the same nanostructures have also been explored as the artificial sieving materials for the separation of biomolecules [22–26]. The initial results were very promising. However, in most cases, these nanostructures were not integrated with the microfluidic system due to their fabrication processes. The integration of these artificial sieving materials with the microfluidic system would enhance their performance by taking the advantages of the existing microfluidic components and techniques. Therefore, it is desirable to develop a monolith integration process to construct size-controlled nanostructure inside the microfluidic system.

Here, we describe a simple approach to construct monolithically integrated periodic porous nanostructures in the microfluidic system using epoxy-based SU-8 photoresist (MicroChem, Newton, MA, USA) for the separation of biomolecules. SU-8 is a class of photoresist, which is widely used for microelectromechanical systems (MEMS) applications. The cured SU-8 photoresist is highly resistant to acids and bases and exhibits excellent mechanical properties and thermal stability. It was shown that the electrokinetic properties of SU-8 were similar to the commercial glass microdevices [27]. Therefore, from the fabrication point of view, it is desirable to construct microfluidic device using SU-8 as the structure materials due to their mechanical and chemical robustness and ease for fabrication. In addition, the patternable property of photoresist would allow fabricating nanostructures at any desired location inside the microfluidic system.

2. Experimental

2.1. Chip fabrication

To fabricate size-controlled porous nanostructures inside the microfluidic channels, a cover slip (Technical Glass Product, Painesville Twp, OH, USA) was used as the substrate. A layer of 15 μm thick cured SU-8 photoresist was used as the base layer. A second layer of SU-8 photoresist was spun on the base layer and then the microchannels were created in the second layer using a standard photolithography process. To fill the microchannel with colloidal solution, the microchannels were temporally sealed by conformal contact with a 5 mm think polydimethylsiloxane (PDMS) slab. Well-ordered colloidal crystals could be grown in the microchannel using evaporation-induced self-assembly process. The colloidal particles used in this experiment were 330 nm silica nanoparticles (Bangs Laboratories, Fisher, IN, USA). To grow colloidal crystals inside the microchannels, a drop of colloidal solution diluted in 1:1 ratio with methanol was placed in the inlet of the microchannels. After the solvent evaporated, the colloidal particles formed close packed colloidal crystals inside the microchannels as shown in Fig. 1a. The formation of well-ordered nanostructures could be clearly seen by their distinct translucent color as reported by several groups [17–21]. The void spaces among the nanoparticles have been used as the sieving materials for the separation of biomolecules where the effective pore size was about 15% of the diameter of the nanoparticles [23–25]. In this experiment, the inverse structures of the col-
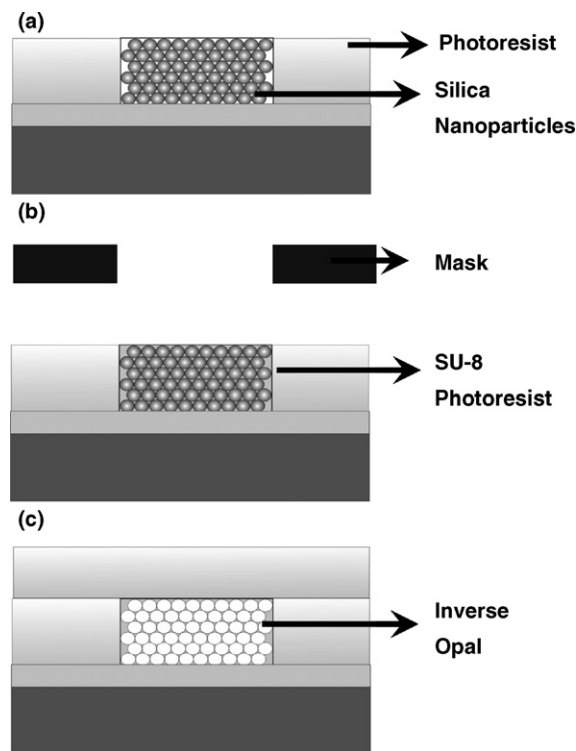

Fig. 1. Schematic for producing well-order periodic nanoporous structure (inverse opal) in the microchannel using SU-8 photoresist. (a) Silica colloidal crystals are first grown inside the SU-8 microchannel. (b) The void spaces of the colloidal crystals are filled with SU-8 photoresist and cured in the desired area using UV radiation. (c) Inverse opal structures can be obtained after removing the silica nanoparticles with BOE solution and sealed with another layer of SU-8 photoresist.

loidal crystals (inverse opal) were used as the sieving medium in the microfluidic channels. To fabricate the inverse opal structure inside the microchannels, the PDMS slab was removed and the void spaces among the colloidal crystals were filled with SU-8 photoresist. A photo-mask and a standard photolithograph process were used to define the location of the inverse opal structures as indicated in Fig. 1b. The inverse opal structure in desired area inside the microfluidic channels could be obtained after photoresist development and subsequent nanoparticle removal by a buffer oxide etch (BOE) solution (6 parts 40% NH_4F and 1 part 49% HF). The microchannels were then sealed by another layer of 50 μm thick SU-8 photoresist (shown in Fig. 1c).

2.2. Sample preparation

To investigate the performance of the well-ordered nanoporous structures as the sieving materials in the integrated microfluidic system, the mobility of two large DNA molecules, λ-phage (MW 48.5 kbp, Sigma) and M13mp18 (MW 7.25 kbp, Sigma), were measured as a function of the applied voltage. To demonstrate the capability of separating biomolecules by such an integrated microdevice, 1 kbp DNA ladder obtained from Violet BioScience was used in this experiment. In both experiments, the DNA molecules were mixed with YOYO-1 dye (nucleic acid dye, trade name, Invitrogen, Carlsbad, CA, USA) at a ratio of 5:1 (base pair/dye) in a 5× Tris borate EDTA buffer (TBE, pH
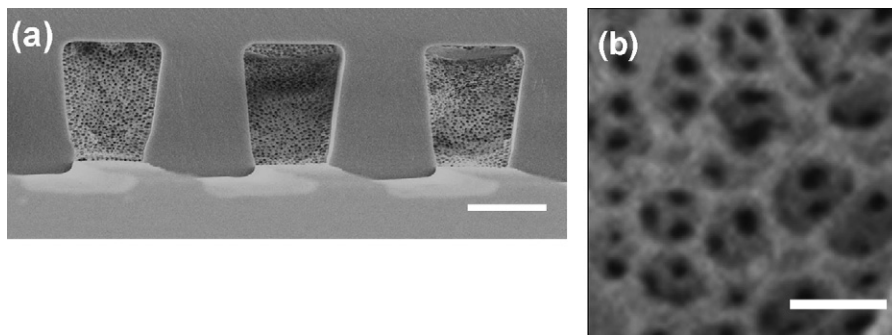
Fig. 2. Cross-sectional SEM images of (a) nanoporous structures inside the microchannels. Bar 4 μm. (b) Enlarged SEM image of the inverse opal structures. Bar 200 nm.

8.3, Sigma–Aldrich). An electrokinetic injection was used to introduce the DNA molecules to the sieving area. The fluorescence images of DNA molecules were taken on an Olympus IX71 inverted microscope equipped with Cascade 512B CCD (charge coupled device) camera (Roper Scientific, Duluth, GA, USA).

3. Results and discussion

3.1. Monolithic integration of SU-8 microchannels

In this experiment, the well-ordered colloidal crystals were used as the templates for making the periodic nanoporous structures inside the microfluidic channels. To see how well the periodic nanoporous structures (inverse opal) can be integrated into the microfluidic channels, several 5 μm (width) × 5 μm (height) microfluidic channels were fabricated on SU-8 photoresist using a standard photolithography process. Following the procedures described in Section 2, nanoporous structures inside the microfluidic channels can be obtained. To investigate the cross-sectional scanning electron microscopy (SEM) image of the microfluidic channels, the microchip was first dipped into liquid nitrogen and cut by a razor blade. Shown in Fig. 2 are the cross-sectional SEM images of the ordered porous nanostructure inside the microchannels. It can be clearly seen that the nanostructures were integrated very well with the microchannels. One advantage of such monolithic integration is that the mechanical strength of the nanostructures is very robust compared to the periodic nanostructured fabricated by colloidal particles. These nanostructures in the microchannel could easily sustain a flow rate up to 2 mm/s driven by a syringe pump, which also indicated that the percentage of defects inside the periodic nanostructure were very small otherwise the flow would be hindered by the defects.

One important issue in the fabrication of the nanoporous sieving materials is the size of the nanopores. Shown in Fig. 2b is the enlarged SEM image of the inverse opal structures. There were two types of nanopores in the inverse opal structure. The larger one was the cavity formed by removing the nanoparticles where the diameter of the cavity was almost the same as the diameter of the nanoparticles. The small one was the interconnecting pores, which were formed due to the close contact between the silica nanoparticles. Despite the fact that the nanostructures were dis-

torted during the cutting process, the periodic interconnecting pores in the second layer can still be seen. The interconnecting pore size was measured to be around 30 nm, which was smaller than those reported previously due to smaller nanoparticles used in experiment [22]. We summarize that using the colloidal crystals, which were formed by 330 nm silica nanoparticles, as templates, we were able to construct periodic pores with a cavity diameter around 300 nm and interconnecting pores around 30 nm.

3.2. Mobility measurement

It has been suggested that the well-ordered nanoporous arrays might be used to separate large DNA molecules because of their unusual size and electric field dependence in the electrophoretic mobility [26]. Since the nanoporous materials fabricated by our approach were composed of 300 nm well-ordered cavities and 30 nm interconnecting pores, it was important to investigate the mobility of large DNA molecules as a function of the applied electric field in the nanoporous materials. Shown in Fig. 3 is the measured electrophoretic mobility of λ-DNA (solid circles) and M13mp18 vector (open circles) in the nanoporous materials. At the lowest applied electric field of 10 V/cm, the mobility of λ-DNA was about $1.9 \times 10^{-4} \, \mathrm{cm^2 \, V^{-1} \, s^{-1}}$,

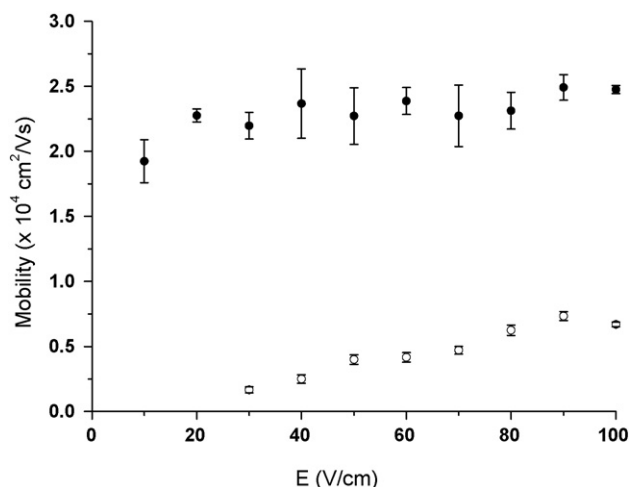Fig. 3. The electrophoretic mobility of λ-DNA (solid circles) and M13mp18 vector (open circles) as a function of the applied electric field.

which was larger than the mobility measured in agarose gel ($\sim0.8 \times 10^{-4}\,cm^2\,V^{-1}\,s^{-1}$) but similar to those measured in the nanoporous materials formed by silica colloidal particles ($\sim1.8 \times 10^{-4}\,cm^2\,V^{-1}\,s^{-1}$) [24]. From Fig. 3, it can be clearly seen that the electrophoretic mobility of the larger λ-DNA molecules in the ordered nanoporous materials is larger than the smaller M13mp18 molecules. However, in agarose gel, larger DNA molecules exhibited smaller electrophoretic mobility. The unusual electrophoretic behavior in the nanoporous materials has been observed before and could be explained by the entropic trapping effect [15]. Since the sizes of the DNA molecules were much larger than the interconnecting pores, DNA molecules have to deform before passing through the interconnecting pores of the nanoporous materials. Larger DNA molecules have higher probability to fit into the interconnecting pores, therefore, exhibiting larger electrophoretic mobility.

3.3. DNA separations

Knowing that the electrophoretic mobility for different sizes of DNA molecules in the nanoporous materials was different, the next step was to utilize the nanoporous structures for sieving biomolecules based on their sizes. Since the porous nanostructure could be integrated into the microchannel, we have designed a DNA separation microdevice where the nanostructures were located at the downstream of a cross-injector as depicted in Fig. 4a. Shown in Fig. 4b is an optical image of a 1 cm long well-ordered nanoporous structures built in a 200 μm wide SU-8 microchannel. After loading DNA ladders in the sample reservoir, the double strain DNA ladders were introduced to the nanoporous area by electrokinetic injection. Shown in Fig. 5 are the fluorescence images of the double strain DNA ladders in both conventional and well-ordered nanoporous separation media. From Fig. 5, it can be clearly seen that all the bands resolved by the conventional agarose gel could be also resolved
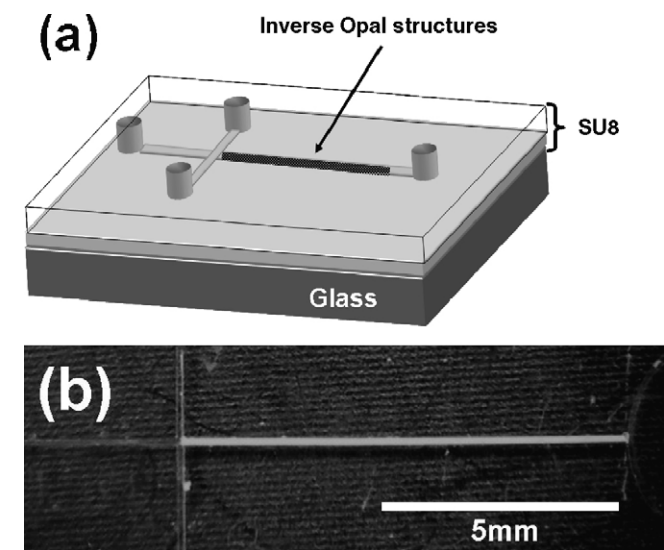

Fig. 4. (a) Layout for the integrated electrokinetic separation system. Glass was used as the support for the system. (b) Optical image of the integrated nanoporous separation system.
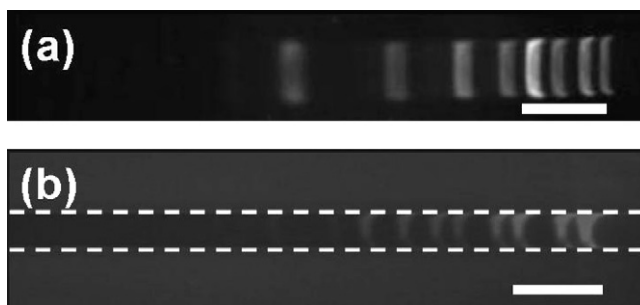

Fig. 5. (a) The fluorescence image of the 1 kbp DNA ladder in a conventional agarose gel. Bar 1 cm. (b) The fluorescence image of the 1 kbp DNA in the microchannel integrated with well-ordered nanoporous structures. The dashed lines represent the microchannel. Bar 500 μm.
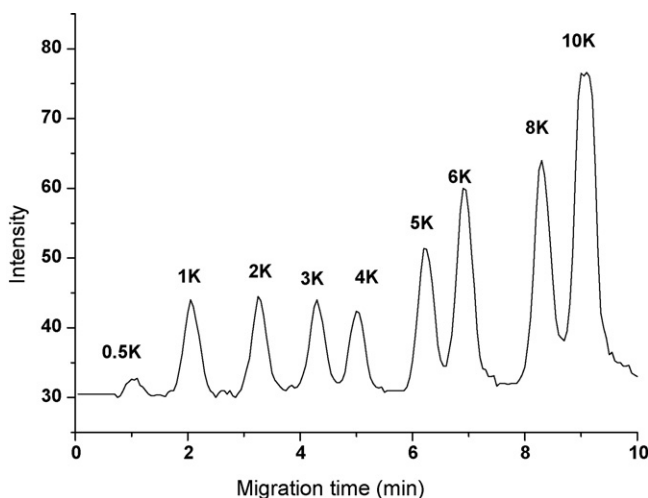

Fig. 6. The electropherogram of the 1 kbp DNA in the microchannel integrated with well-ordered nanoporous structures. Electric field: 20 V/cm.

in the microchannel with nanoporous structures as the separation component.

At the electric field of $20\,V\,cm^{-1}$, it took less than 10 min to separate 1 kbp ladder. Shown in Fig. 6 is the electropherogram of DNA ladders in the integrated microchannels with 2.5 mm separation distance. Similar results were obtained when different batches of microchips were used. We conclude that it is possible to integrate the periodic nanoporous structures into the microchannel for separating DNA molecules.

4. Conclusions

In summary, the solvent evaporation induced self-assembly process was used to produce well-order silica colloidal crystals inside the microfluidic channels made by SU-8 photoresist. By filling the void space with SU-8 photoresist, curing and subsequent nanoparticle removal, monolithic integration of nanoporous materials inside the microfluidic channels has been achieved. The interconnecting pore size of the nanoporous structures was measured to be around 30 nm where as the cavity size was around 300 nm. It was observed that the electrophoretic mobility of the larger λ-DNA molecules was larger than the smaller M13mp18 molecules. Such an integrated nanoporous

C.-W. Kuo et al. / J. Chromatogr. A 1162 (2007) 175–179

179

system was used to separate 1 kbp DNA ladder within 10 min. Since the SU-8 photoresist is resistant various solvents, the monolithic fabrication of nanoporous materials in the SU-8 microfluidic system provides a great opportunity to separate various chemical molecules and biological molecules on an integrated microdevice.

Acknowledgements

References

[1] J.H. Ng, L.L. Ilag, Biotechnol. Ann. Rev. 9 (2003) 1.
[2] P. Mitchell, Nat. Biotechnol. 19 (2001) 717.
[3] G.H.W. Sanders, A. Manz, Trends Anal. Chem. 19 (2000) 364.
[4] E. Delamarche, A. Bernard, H. Schmid, A. Bietsch, B. Michel, H.J. Biebuyck, J. Am. Chem. Soc. 120 (1998) 50.
[5] M.U. Kopp, A.J. Mello, A. Manz, Science 280 (1998) 1046.
[6] M.J. Wirth, Anal. Chem. 79 (2007) 801.
[7] C.W. Kan, C.P. Fredlake, E.A.S. Doherty, A.E. Barron, Electrophoresis 25 (2004) 3564.
[8] S. Yao, D.S. Anex, W.B. Caldwell, D.W. Anold, K.B. Smith, P.G. Schultz, Proc. Natl. Acad. Sci. USA 96 (1999) 5372.
[9] A.E. Herr, A.K. Singh, Anal. Chem. 76 (2004) 4727.
[10] C.F. Chou, O. Bakajin, S.W.P. Turner, T.A.J. Duke, S.S. Chan, E.C. Cox, H.G. Craighead, R.H. Austin, Proc. Natl. Acad. Sci. USA 96 (1999) 13762.
[11] L.R. Huang, J.O. Tegenfeldt, J.J. Kraeft, J.C. Sturn, R.H. Austin, E.C. Cox, Nat. Biotechnol. 20 (2002) 1048.
[12] J. Fu, P. Mao, J. Han, Appl. Phys. Lett. 87 (2005) 263902.
[13] L.R. Huang, E.C. Cox, R.H. Austin, J.C. Sturm, Science 304 (2004) 987.
[14] J. Han, S.W. Turner, H.G. Craighead, Phys. Rev. Lett. 83 (1999) 1688.
[15] J. Fu, J. Yoo, J. Han, Phys. Rev. Lett. 97 (2006) 018103.
[16] P. Jiang, J.F. Bertone, K.S. Hwang, V.L. Colvin, Chem. Mater. 11 (1999) 2132.
[17] S.M. Yang, G.A. Ozin, Chem. Commun. 24 (2000) 2507.
[18] S.M. Yang, H. Miguez, G.A. Ozin, Adv. Funct. Mater. 12 (2002) 425.
[19] G.A. Ozin, S.M. Yang, Adv. Funct. Mater. 11 (2001) 95.
[20] J.Y. Shiu, C.W. Kuo, P. Chen, J. Am. Chem. Soc. 126 (2004) 8096.
[21] J.Y. Shiu, P. Chen, Adv. Mater. 17 (2005) 1866.
[22] D. Nykypanchuk, H.H. Strey, D.A. Hoagland, Science 297 (2002) 987.
[23] M. Tabuchi, M. Ueda, N. Kaji, Y. Yamasaki, Y. Nagasaki, K. Yoshikawa, K. Kataoka, Y. Baba, Nat. Biotechnol. 22 (2004) 337.
[24] H. Zhang, M.J. Wirth, Anal. Chem. 77 (2005) 1237.
[25] S. Zheng, E. Ross, M.A. Legg, M.J. Wirth, J. Am. Chem. Soc. 128 (2006) 9016.
[26] Y. Zeng, D.J. Harrison, Electrophoresis 27 (2006) 3747.
[27] T. Sikanen, S. Tuomikoski, R.A. Ketola, R. Kostiainen, S. Franssila, T. Kotiaho, Lab Chip 5 (2005) 888.